

Molecularly Imprinted Silica Nanospheres Embedded CdSe Quantum Dots for Highly Selective and Sensitive Optosensing of Pyrethroids

Haibing Li,* Yuling Li, and Jing Cheng

Key Laboratory of Pesticide and Chemical Biology (CCNU), Ministry of Education,
College of Chemistry, Central China Normal University, Wuhan 430079, P.R. China

Received September 12, 2009. Revised Manuscript Received March 2, 2010

This paper reports the molecularly imprinted polymer (MIP)-based fluorescence nanosensor which is developed by anchoring the MIP layer on the surface of silica nanospheres embedded CdSe quantum dots (QDs) via a surface molecular imprinting process. The molecularly imprinted silica nanospheres (CdSe@SiO₂@MIP) were characterized by scanning electron microscopy (SEM), transmission electron microscopy (TEM), IR spectroscopy, and so forth, which demonstrated the formation of uniform core–shell lambda-cyhalothrin(LC)-imprinted silica nanospheres. The synthesized CdSe@SiO₂@MIP shows higher photostability, and allows a highly selective and sensitive determination of LC via FL intensity decreasing when removal of the original templates. The CdSe@SiO₂@MIP was applied to detect trace LC in water without the interference of other pyrethroids and ions. Under optimal conditions, the relative FL intensity of CdSe@SiO₂@MIP decreased linearly with the increasing LC in the concentration in the range of 0.1–1000 μM with a detection limit (3σ) of 3.6 μg·L⁻¹. It is found that LC can quench the luminescence of CdSe@SiO₂@MIP in a concentration-dependent manner that is best described by a Stern–Volmer-type equation. The possible mechanism is discussed.

Semiconductor quantum dots (QDs) as high luminescence nanocrystals has attracted considerable attention in recent years, owing to their unique optical and electronic properties,^{1,2} such as sharp emission band with broad excitation, and strong resistance to photobleaching. Since Chen and Rosenzweig reported the first practical use of CdS QDs as chemical sensors to determine Zn(II) and Cu(II) ions in aqueous media,³ a number of QD-based sensors have been reported.^{4–10} For instance, Chen and co-workers have synthesized 15-crown-5 functionalized

CdSe/ZnS QDs as a sensing unit toward K⁺ in aqueous solution.⁴ We reported that cyclodextrin modified CdSe/ZnS QDs allowed a highly sensitive determination of environmental pollutant phenols.⁶ Recently, Johnson and co-worker have developed a single QD-based aptameric sensor that is capable of sensing the presence of cocaine.⁷ Owing to the sustained interest of selective chemo-sensor in environmental monitoring, the design of sensing devices based on QDs is a topic of great interest.

In general, surface functionalization is a key to fabricate QD-based probes because of surface modification affording not only the excellent stability of the QDs but also the desired surface binding sites. Among the numerous modifications for QDs, the incorporation of QDs in silica has received considerable attention in the past few years.^{11–15} Silica is a good option for the inert material,

*To whom correspondence should be addressed. E-mail: hbing@mail.ccnu.edu.cn. Phone: 86-27-67866423.

(1) (a) Bruchez, M.; Moronne, M.; Cin, P.; Weiss, S.; Alivisatos, A. P. *Science* **1998**, *281*, 2013–2015. (b) Chan, W. C. M.; Nie, S. *Science* **1998**, *281*, 2016–2018.

(2) (a) Dubertret, B.; Skourides, P.; Norris, D. J.; Noireaux, V.; Brivanlou, A. H. *Science* **2002**, *298*, 1759–1762. (b) Larson, D. R.; Zipfel, W. R.; Williams, R. M.; Clark, S. W.; Bruchez, M. P.; Wise, F. W.; Webb, W. W. *Science* **2003**, *300*, 1434–1436.

(3) Chen, Y. F.; Rosenzweig, Z. *Anal. Chem.* **2002**, *74*, 5132–5138.

(4) Chen, C. Y.; Cheng, C. T.; Lai, C. W.; Wu, P. W.; Wu, K. C.; Chou, P. T.; Chouh, Y. H.; Chiu, H. T. *Chem. Commun.* **2006**, *3*, 263–265.

(5) (a) Ruedas-Rama, M. J.; Hall, E. A. H. *Anal. Chem.* **2008**, *80*, 8260–8268. (b) Gattás-Asfura, K. M.; Leblanc, R. M. *Chem. Commun.* **2003**, *21*, 2684–2685. (c) Jin, W. J.; Costa-Fernández, J. M.; Pereiro, R.; Sanz-Medel, A. *Anal. Chim. Acta* **2004**, *522*, 1–8.

(6) Li, H. B.; Han, C. P. *Chem. Mater.* **2008**, *20*, 6053–6059.

(7) Zhang, C. Y.; Johnson, L. W. *Anal. Chem.* **2009**, *81*, 3051–3055.

(8) (a) Riu, J.; Maroto, A.; Rius, F. X. *Talanta* **2006**, *69*, 288–301. (b) Wolfbeis, O. S. *J. Mater. Chem.* **2005**, *15*, 2657–2669. (c) Freeman, R.; Finder, T.; Bahshi, L.; Willner, I. *Nano Lett.* **2009**, *9*, 2073–2076.

(9) (a) Xu, X. H.; Yeung, E. S. *Science* **1997**, *275*, 1106–1109. (b) Hsin, T. M.; Yeung, E. S. *Angew. Chem., Int. Ed.* **2007**, *46*, 8032–8035. (c) Sharonov, A.; Hochstrasser, R. M. *Biochemistry* **2007**, *46*, 7963–7972.

(10) (a) Shi, L. F.; Paoli, V. D.; Rosenzweig, N.; Rosenzweig, Z. *J. Am. Chem. Soc.* **2006**, *128*, 10378–10379. (b) Zhang, C. Y.; Johnson, L. W. *J. Am. Chem. Soc.* **2008**, *130*, 3750–3751.

(11) Darbandi, M.; Thomann, R.; Nann, T. *Chem. Mater.* **2005**, *17*, 5720–5725.

(12) (a) Koole, R.; Schooneveld, M. M.; Hilhorst, J.; Castermans, K.; Cormode, D. P.; Strijkers, G. J.; Donega, C. M.; Vanmaekelbergh, D.; Griffoen, A. W.; Nicolay, K. F. Z. A.; Meijerink, A.; Mulder, W. J. M. *Bioconjugate Chem.* **2008**, *19*, 2471–2479. (b) Nann, T.; Mulvaney, P. *Angew. Chem., Int. Ed.* **2004**, *43*, 5393–5396.

(13) (a) Yi, D. K.; Selvan, T.; Lee, S. S.; Papaefthymiou, G. C.; Kundaliya, D.; Ying, J. Y. *J. Am. Chem. Soc.* **2005**, *127*, 4990–4991. (b) Arduini, M.; Mancin, F.; Tecilla, P.; Tonellato, U. *Langmuir* **2007**, *23*, 8632–8636.

(14) Tan, T. T.; Selvan, S. T.; Zhao, L.; Gao, S. J.; Ying, J. Y. *Chem. Mater.* **2007**, *19*, 3112–3117.

(15) (a) Correa-Duarte, M. A.; Giersig, M.; Liz-Marzán, L. M. *Chem. Phys. Lett.* **1998**, *286*, 497–501. (b) Gerion, D.; Pinaud, F.; Williams, S. C.; Parak, W. J.; Zanchet, D.; Weiss, S.; Alivisatos, A. P. *J. Phys. Chem. B* **2001**, *105*, 8861–8871. (c) Song, Y. Y.; Cao, X. B.; Guo, Y.; Chen, P.; Zhao, Q. R.; Shen, G. Z. *Chem. Mater.* **2009**, *21*, 68–77.

since it impedes the diffusion of charge carriers generated upon photoexcitation as well as the diffusion of oxygen from the environment.¹⁶ Furthermore, silica with a highly cross-linked rigid matrix is ideally suitable for the formation of delicate recognition sites. For example, in our recent study, we synthesized CdTe nanocrystals in sol-gel-derived composite silica spheres coated with calix[4]-arene as fluorescent sensors for carbamates pesticides.¹⁷ As we know, a promising way to achieve the tailored selectivity of analytes is the use of molecularly imprinted polymers (MIPs). Molecular imprinting is a technique to make a selective binding site for a specific chemical. The stability, ease of preparation, and low cost make the molecularly imprinted materials particularly attractive.^{18–20} Zhang and co-workers have synthesized of 2,4,6-trinitrotoluene(TNT)-imprinted silica nanoparticles with a high density of absorption for TNT.¹⁸ Yan and co-worker have reported the surface molecular imprinting on Mn-doped ZnS quantum dots for room-temperature phosphorescence optosensing of pentachlorophenol.²¹ It is reasonable to believe that molecular imprinting technique will be a powerful tool to introduce artificial receptor moieties onto the surface of silica spheres. Because of our continued interest in silica nanosphere-based sensors, imprinting the template molecule on the shell of the SiO₂ encapsulated QDs to develop the new sensing materials is studied in our laboratory. As far as we know, MIP-based QDs nanosensors for fluorescent responding of pyrethroids are almost unexplored.

In agricultural situations, pyrethroids are used for the control of a wide range of pests.²² In recent years, the use of pyrethroids is increasing in place of highly toxic insecticides such as organochlorines and organophosphorus insecticides.²³ However, pyrethroids are known to cause disturbed consciousness and seizures by affecting the central nervous system of humans and are also suspected to have endocrine-disrupting effects. Therefore, maximum residue limits for pyrethroid residues set by the U.S. Environment Protection Agency (EPA) are not more than 0.05 $\mu\text{g g}^{-1}$.²⁴ Thus, analytical techniques

with high sensitivity and selectivity are developed to monitor pyrethroids poisoning. Pyrethroids detecting techniques mostly focus on chromatography separation, such as high performance liquid chromatography (HPLC), gas chromatography (GC), coupled column liquid chromatography/mass spectrometry, and so forth.²⁵ However, these methods are time-consuming and require a tedious sample pretreatment. Thus, the development of simple and rapid pyrethroid detecting methods presents a challenge.

In this article, we report the formation of molecular recognition sites on the surface of silica nanospheres embedded QDs. When the template was removed by solvent extraction, the MIP-based silica nanospheres are capable of selectively rebinding the target molecule lambda-cyhalothrin (LC). Under optimal conditions, the relative FL intensity is decreased linearly with the increase in the concentration of LC in the range of 0.1–1000 μM with a detection limit of 3.6 $\mu\text{g L}^{-1}$. Herein, the silica nanospheres embedded CdSe QDs with MIP optosensing protocol were demonstrated for simple, rapid, and selective detection of trace LC in water.

Experimental Section

Cadmium oxide (99.99%), trioctylphosphine oxide (TOPO, 99%), trioctylphosphine (TOP, 90%), selenium (powder, 99.99%), anhydrous chloroform were purchased from Aldrich (Milwaukee, WI, U.S.A.). Hexylphosphonic acid (HPA) was obtained from Alfa Aesar (Karlsruhe, Germany). 3-Aminopropyltriethoxysilane (APTS) and tetraethoxysilane (TEOS) were obtained from the Chemical Plant of Wuhan University. TritonX-100-(*t*-octylphenoxyethoxyethanol) and aqueous ammonia solution are purchased from Shanghai Chemical Factory, China. Pyrethroids standards (lambda-cyhalothrin, cypermethrin (CM), permethrin(PM), deltamethrin(DM)) studied were provided by the Key Laboratory of Pesticide and Chemical Biology (CCNU), Ministry of Education, China. All pesticides standards are of 98–99% purity. Pyrethroids are dissolved in ethanol and diluted with water for storage at room temperature.

Characterizations. FL spectra are taken on a Fluoromax-P luminescence spectrometer (Horiba Jobin Yvon Inc.). IR spectra are measured with a NEXUS FT/IR spectrometer (Thermo Nicolet Co.). Scanning electron microscopy (SEM) images were recorded by JEOL 6700-F. Transmission electron microscopy (TEM) were recorded by a JEOL-JEM 2010 electron microscope operating at 200 kV. The samples are dropped onto a small copper mesh and left at room temperature so that the samples precipitate homogeneously on the carbon films among the tiny pores of the copper mesh. The average particle size (z-average size) and size distribution are measured by photon correlation spectroscopy (Nano ZS90 zetasizer, Malvern Instruments Corp, U.K.) at 25 °C under a fixed angle of 90° in disposable polystyrene cuvettes. The measurements are obtained using a He–Ne laser of 633 nm. No multiscattering phenomenon is observed.

Preparation of CdSe QDs. Trioctylphosphine oxide(TOPO)-capped CdSe QDs were synthesized using CdO as precursor via the procedure described by Peng's group,²⁶ although some slight modifications were made here. Briefly, 0.03 g of CdO (0.233 mmol),

- (16) Yang, Y. H.; Gao, M. Y. *Adv. Mater.* **2005**, *17*, 2354–2357.
- (17) Li, H. B.; Qu, F. G. *Chem. Mater.* **2007**, *19*, 4148–4154.
- (18) Gao, D. M.; Zhang, Z. P.; Wu, M.; Xie, C. G.; Guan, G.; Wang, D. P. *J. Am. Chem. Soc.* **2007**, *129*, 7859–7866.
- (19) (a) Haupt, K.; Mosbach, K. *Chem. Rev.* **2000**, *100*, 2495–2504. (b) Zimmerman, S. C.; Wendland, M. S.; Rakow, N. A.; Zharov, I.; Suslick, K. S. *Nature* **2002**, *418*, 399–403. (c) Mertz, E.; Zimmerman, S. C. *J. Am. Chem. Soc.* **2003**, *125*, 3424–3425. (d) Katz, A.; Davis, M. E. *Nature* **2000**, *403*, 286–289. (e) Bass, J. D.; Katz, A. *Chem. Mater.* **2003**, *15*, 2757–2763.
- (20) Xie, C. M.; Liu, B. H.; Wang, Z. Y.; Gao, D. M.; Guan, G. J.; Zhang, Z. P. *Anal. Chem.* **2008**, *80*, 437–443.
- (21) Wang, H. F.; He, Y.; Ji, T. R.; Yan, X. P. *Anal. Chem.* **2009**, *81*, 1615–1621.
- (22) *The agrochemical handbook*, 3rd ed.; Kidd, H., James, D. R., Eds.; The Royal Society of Chemistry: Cambridge, 1991.
- (23) (a) Hadfield, S. T.; Sadler, J. K.; Bolygo, E.; Hill, I. R. *Pestic. Sci.* **1992**, *35*, 45–57. (b) Oudou, H. C.; Alonso, R. M.; Bruun Hansen, H. C. *Anal. Chim. Acta* **2004**, *523*, 69–74. (c) Oudou, H. C. *Analysis and sorption of pyrethroids in soil environments*; Ph.D. Thesis, University of Copenhagen KVL, Copenhagen, Denmark, 2002; p 50.
- (24) (a) Barro, R.; Garcia-Jares, C.; Llompart, M.; Cela, R. *J. Chromatogr. Sci.* **2006**, *44*, 430–437. (b) Reigart, J. R.; Roberts, J. R. *Recognition and Management of Pesticide Poisonings*, 5th ed.; U.S. Environment Protection Agency (EPA): Washington, DC, 1999.
- (25) Cheng, J. H.; Liu, M.; Yu, Y.; Wang, X. P.; Zhang, H. Q.; Ding, L.; Jin, H. Y. *Meat Sci.* **2009**, *82*, 407–412.
- (26) Qu, L.; Peng, X. *J. Am. Chem. Soc.* **2002**, *124*, 2049–2055.

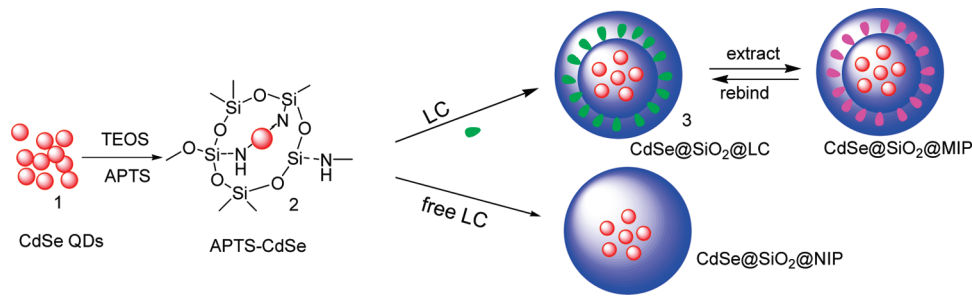


Figure 1. Schematic illustration for the molecular imprinting process of LC-imprinted silica nanospheres embedded CdSe quantum dots.

0.11 g of HPA, and 3.5 g of TOPO were mixed to heat at 300–320 °C under argon flow for 15–20 min, and CdO was dissolved in HPA and TOPO. The solution of selenium-TOP was swiftly injected, and a change of solution color to red was observed. After injection, CdSe nanoparticles were left to grow for about 20 min at 250 °C. When the CdSe nanoparticles were formed, the solution was cooled to 100 °C. The CdSe QDs were precipitated by addition of methanol and separated by centrifugation. To remove excess TOPO molecules, the QD precipitates were dissolved in chloroform again and precipitated by addition of methanol. This procedure was repeated three times. We also synthesized the TOPO-capped CdSe QDs with different emissions by this method. The fluorescence spectra and UV–vis spectra of CdSe QDs with different emissions can be seen in the Supporting Information, Figure S1. Generally, we chose the CdSe QDs with emission peaks at 610 nm for the future experiments.

Preparation of LC Imprinting in Silica Nanospheres Embedded QDs (CdSe@SiO₂@MIP). LC-imprinted silica nanospheres embedded CdSe quantum dots were synthesized by the modified reverse microemulsion methods.²⁷ Typically, 1.8 mL of TritonX-100 was dispersed in 7.5 mL of cyclohexane and stirred for 15 min. Subsequently, 400 μL CdSe QDs (1 mg mL⁻¹) dispersed in chloroform, 50 μL of TEOS, and 100 μL of ammonia were added. When the mixture was stirred for 2 h, 20 μL of APTS-CdSe and 5 mg of LC dispersed in cyclohexane (0.2 mL) were added, and the mixture was stirred overnight. Finally, the CdSe@SiO₂@LC was purified by adding 10 mL of acetone to the reaction mixture and centrifuged for 10 min. After removal of the supernatant, 3 mL of water was added, and the silica particles were reagentized again by centrifugation for 20 min.

Original LC templates in the imprinted shells of core–shell silica nanoparticles were extracted with a mixture solvent of ethanol/acetonitrile (v/v, 8:2). This was repeated once more for 40 min after CdSe@SiO₂@LC were redispersed in ethanol. After removal of the templates, the steady-state binding capacity of CdSe@SiO₂@MIP (10 μg mL⁻¹) was measured with different LC concentrations by fluorescence spectroscopy.

Preparation of Nonimprinting Silica Nanospheres Embedded QDs (CdSe@SiO₂@NIP). Nonimprinted nanoparticles (NIPs) CdSe@SiO₂@NIP as a control to evaluate the molecular recognition properties of imprinted materials were synthesized similar to the CdSe@SiO₂@MIP via the reverse microemulsion method. To obtain a more precise comparison with imprinted nanoparticles, an equal amount of APTS monomers was also used in the synthesis system of the NIPs. After being purified by centrifugation, the CdSe@SiO₂@NIP was dispersed in ethanol for future experiment (10 μg mL⁻¹). We also found that the

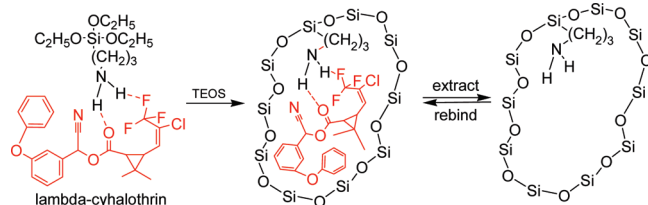


Figure 2. Schematic illustration for the molecular imprinting mechanism of LC in a silica matrix through the hydrogen bond reaction.

reverse microemulsion method is general because of CdSe QDs with different emission (emission peaks of original CdSe QDs at 580 or 610 nm), and obtain the CdSe@SiO₂@NIP with different emission finally that can be seen in the Supporting Information, Figure S2.

Results and Discussion

Of polymeric materials, silica with a highly rigid matrix and hydrophilic surface has a wide choice of functional precursors and structural forms, which makes it ideally suitable for imprinting various organic or biological molecules.²⁴ In this work, 3-aminopropyltriethoxysilane (APTS) was used as a functional monomer to imprint LC molecules. Figure 1 illustrates the major steps involved in the imprinting synthesis on the surface of silica nanospheres. In the first step, CdSe QDs (1) were chemically modified with APTS according to the reported method.¹⁸ The resultant APTS-CdSe (2) was further reacted with LC through hydrogen bond interactions driving template molecules into the formed silica matrix as shown in Figure 2. The silica nanospheres were simply fabricated by means of the hydrolysis and condensation reaction of APTS and TEOS in the presence of aqueous ammonia solution as the catalyst.²⁵ LC templates were assembled and immobilized into the matrix of silica by the silanization reaction between APTS and TEOS to form core–shell CdSe@SiO₂@LC nanospheres (3). After the templates were extracted from the silica matrix by using solvent to decompose the hydrogen bond, the LC-imprinted sites with the covalently anchored amino groups at the cavity were created in the silica matrix (Figure 2). Finally, after the LC was removed from the silica shells with solvent extraction, the core–shell CdSe@SiO₂@MIP (4) was obtained.

As can be seen from Figure 3, a distinct difference is found in the fluorescence spectra of the original CdSe QDs, CdSe@SiO₂@NIP, and CdSe@SiO₂@MIP in the

(27) Koole, R.; Schooneveld, M. M.; Hilhorst, J.; Donegá, C. M.; C. T. Hart, D.; Blaaderen, A.; Vanmaekelbergh, D.; Meijerink, A. *Chem. Mater.* **2008**, 20, 2053–2512.

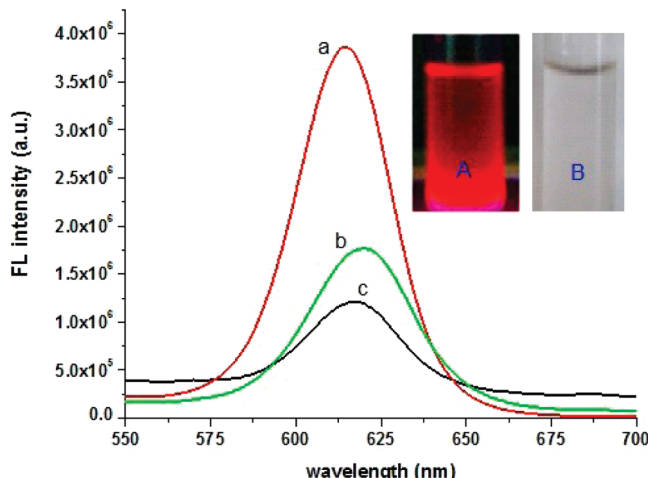


Figure 3. Photoluminescence spectra of (a) the CdSe QDs in chloroform, (b) CdSe@SiO₂@MIP, and (c) CdSe@SiO₂@NIP. Inset: fluorescence photographs of CdSe@SiO₂@MIP in water (A) under UV light irradiation ($\lambda = 365$ nm) and (B) under room light.

positions and FL intensity. Though the FL intensity partly decreases during the preparation process in comparison with that of the original CdSe QDs, the CdSe@SiO₂@NIP and CdSe@SiO₂@MIP still show very bright FL (as indicated by the inset photographs in Figure 3) with a quantum yield (QY) up to 15.6% and 20.1%, respectively, by using Rhodamine B as a criterion (QY = 89%, EtOH) at room temperature. The QY measurement of CdSe@SiO₂@MIP is reliable, and the precision for five replicate detections of CdSe@SiO₂@MIP was 3.2% (RSD). It is by far higher than that of the core–shell silica spheres for only 7% reported by Gao and co-workers.²⁰ As shown in Figure 3, the fluorescence of CdSe@SiO₂@MIP is a slight red-shift in comparison with that of CdSe QDs. It is known that a single charge (Si–O- groups, hydroxyl ions, or ammonium ions) close to the QD surface can generate an electric field that is sufficiently large to cause significant quenching²⁸ and a red-shift²⁹ of the QD emission. Thus, this slight red shift of CdSe@SiO₂@MIP is ascribed to the attachment of fully hydrolyzed and subsequently condensed TEOS (i.e., silica) to the QD surface.²⁹

The TEM images of original CdSe QDs and CdSe@SiO₂@MIP are shown in Figures 4A and 4B, respectively. Figure 4B shows that the CdSe@SiO₂@MIP exhibit single particle features, and the diameters are increased after coating with silica as compared to original CdSe QDs. The average sizes of CdSe@SiO₂@MIP nanoparticles are measured by photon correlation spectroscopy (PCS) about 90 nm (see the Supporting Information). Compared with CdSe@SiO₂@NIP and CdSe@SiO₂@LC as shown in the Supporting Information, Figure S3, the imprinted process does not change the core–shell structure; CdSe@SiO₂@MIP still obtain with the uniform core–shell LC-imprinted silica nanospheres (Figure 4B). As shown in the SEM images of Figure 4C, the CdSe@SiO₂@MIP show highly spherical morphology and rough

surface, which is different from that of CdSe@SiO₂@NIP.

The IR spectra of CdSe@SiO₂@NIP, CdSe@SiO₂@LC, and CdSe@SiO₂@MIP can confirm the successful imprinting of LC to the surface of silica in Figure 5. The IR data contain features identified on CdSe@SiO₂@LC, as shown in Figure 4b: the peaks for ester of LC at 1733 cm⁻¹, and the peaks in the benzene ring stretching at 1454 cm⁻¹. The width peak from 1000 to 1100 cm⁻¹ is the characteristic peaks of Si–O–Si. After solvent extraction, these characteristic peaks of LC disappear in the IR spectrum of CdSe@SiO₂@MIP (Figure 5c), which suggests that the LC is successfully imprinted into the silica nanospheres.

The effect of pH in a range between 1 and 13 was studied for CdSe@SiO₂@MIP (black squares) and CdSe@SiO₂@NIP (red circles) in Figure 6. The FL intensity of CdSe@SiO₂@MIP in the interval 4.0–10 is considerably stable. However, the FL intensity decreases quickly in acidic or strong basic media. Clearly at low pH, the surface of the CdSe@SiO₂@MIP is possible being dissolved, resulting in surface defects. In a pH medium below 3, the luminescence emission has been completely quenched. As pH is increased from 11 to 13, the FL intensity decreases quickly, because silica shell can be ionized at high pH, and OH⁻ could nucleophilically attack the surface and create surface defects. Finally, a pH of 7.0 is selected for further experiments.

The stabilities of CdSe@SiO₂@NIP and CdSe@SiO₂@MIP are estimated at room temperature, as shown in Figure 7. It is found that the FL intensity of the CdSe@SiO₂@MIP is increased gradually in 6 days. After that, the FL intensity decreases in the next 6 days, and then the FL intensity is held. The similar phenomenon was observed for the photostability of CdSe@SiO₂@NIP. Thus, generally, the CdSe@SiO₂@MIP can be stable for nearly 1 month.

The aim of the present study is to determinate the selectivity and sensitivity of pyrethroids by the CdSe@SiO₂@MIP. The fluorescence response of CdSe@SiO₂@MIP toward various pyrethroids was conducted to examine the selectivity. As shown in Figure 8, only LC shows strong fluorescence quenching of CdSe@SiO₂@MIP, which is also displayed in inset fluorescence photographs of Figure 8. But for CdSe@SiO₂@NIP, all pyrethroids have very little effect. The fluorescence titration of CdSe@SiO₂@MIP with common anion and ion was conducted to examine the interference of ions. As shown in Table 1, the interference of alkali, alkali earth ions and anions, such as Na⁺, K⁺, Mg²⁺, Ca²⁺, halogen anions, NO₃⁻, CO₃²⁻, and so forth have basically no effect on FL intensity of CdSe@SiO₂@MIP. The fluorescence analysis of CdSe@SiO₂@MIP with the mixed pyrethroids was made to examine the interference of other pyrethroids. As shown in Figure 9, the interference of cypermethrin, beta-cyfluthrin, permethrin, and deltamethrin are very weak and can be ignored. Therefore, CdSe@SiO₂@MIP can be used for highly selective and sensitive analysis of LC in the presence of other commonly interfering ions and

(28) Wang, L. W. *J. Phys. Chem. B* **2001**, *105*, 2360–2364.

(29) Empedocles, S. A.; Bawendi, M. G. *Science* **1997**, *278*, 2114–2117.

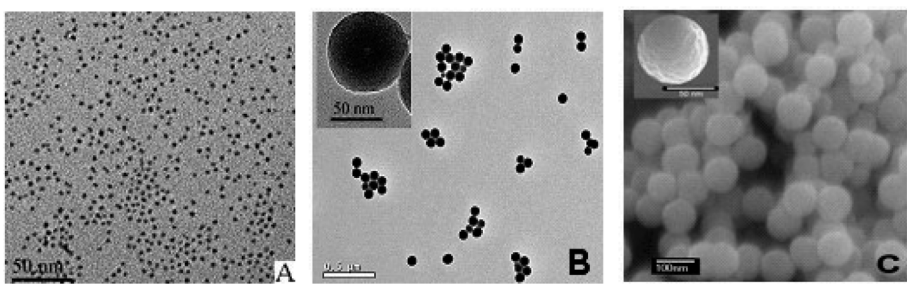


Figure 4. TEM images of (A) original CdSe QDs (scale bar: 50 nm), (B) CdSe@SiO₂@MIP (scale bar: 500 nm), inset: TEM image of a single CdSe@SiO₂@MIP particle (scale bar: 50 nm). (C) SEM image of CdSe@SiO₂@MIP (scale bar 100 nm), inset: SEM image of a single CdSe@SiO₂@MIP particle (scale bar: 50 nm).

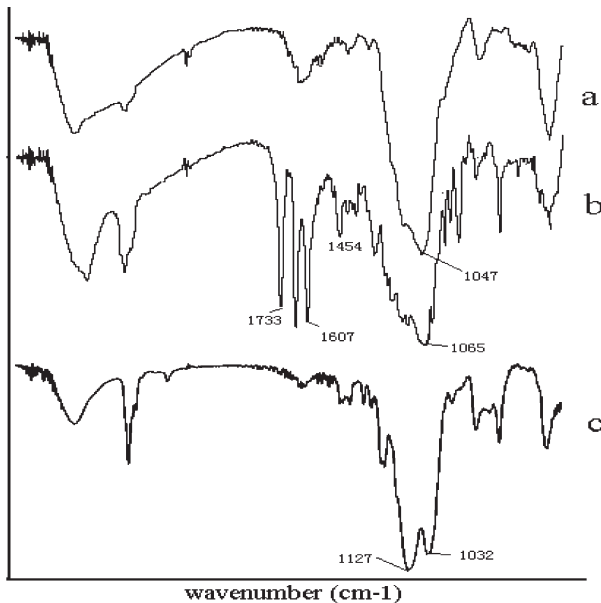


Figure 5. FT-IR spectra of (a) CdSe@SiO₂@NIP, (b) CdSe@SiO₂@LC, and (c) CdSe@SiO₂@MIP.

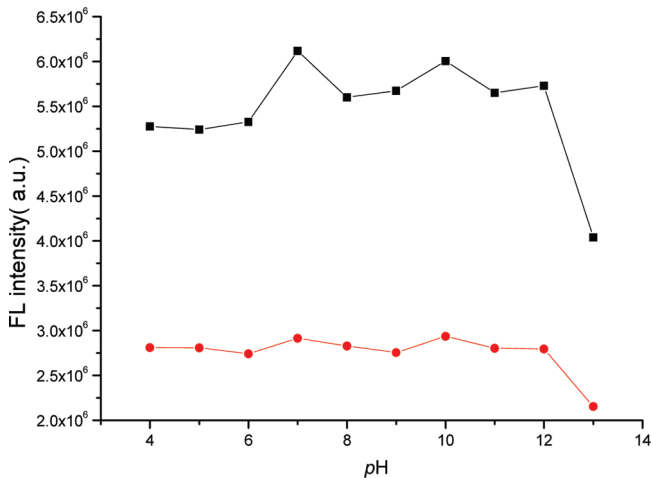


Figure 6. Effect of pH on luminescence of the CdSe@SiO₂@MIP (black squares) and CdSe@SiO₂@NIP (red circles).

pyrethroids. The above results reveal that CdSe@SiO₂@MIP shows a much higher selectivity for LC. It is reasonable that the imprinted binding sites (cavities) play an important role in the selective luminescence response to LC. It is known that the well-defined structure of the imprinted cavities can be exploited for the rebinding of

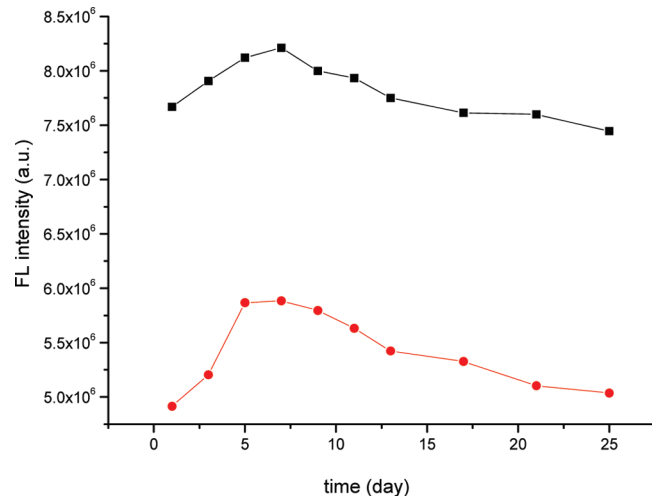


Figure 7. Photostability of CdSe@SiO₂@MIP (black squares) and CdSe@SiO₂@NIP (red circles).

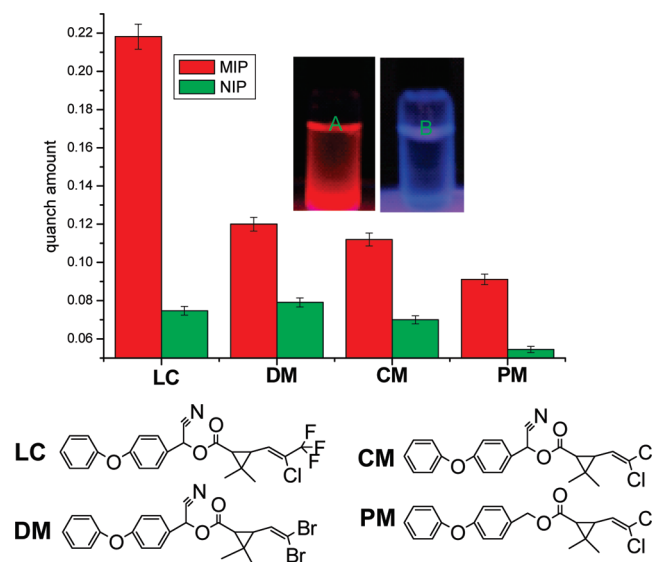


Figure 8. Top: quenching amount of CdSe@SiO₂@MIP and CdSe@SiO₂@NIP by different kinds of 0.5 mmol L⁻¹ pyrethroids (LC, DM, CM, and PM). Inset: (A) fluorescence photographs of CdSe@SiO₂@MIP, (B) CdSe@SiO₂@MIP + LC (under $\lambda = 365$ nm UV light irradiation). Bottom: the molecular structure of different pyrethroids.

template molecules. However, the imprinted cavity of CdSe@SiO₂@MIP is not suitable to accommodate the other pyrethroids, which results in the selective FL response to LC. The LC can act as an efficient hole or electron

Table 1. Test for the Interference of Different Ions on the Fluorescence of CdSe@SiO₂@MIP^a

coexisting substance	coexisting concentration (10^{-7} mol L $^{-1}$)	change of fluorescence intensity (%)
K $^{+}$	500	+1.8
Na $^{+}$	500	+2.0
Ca $^{2+}$	200	-2.5
Mg $^{2+}$	200	-2.7
CO ₃ $^{2-}$	100	+2.0
NO ₃ $^{-}$	200	+3.0

^a Concentration of lambda-cyhalothrin: 10 $^{-5}$ mol L $^{-1}$. Other conditions are the same as those described in the procedure.

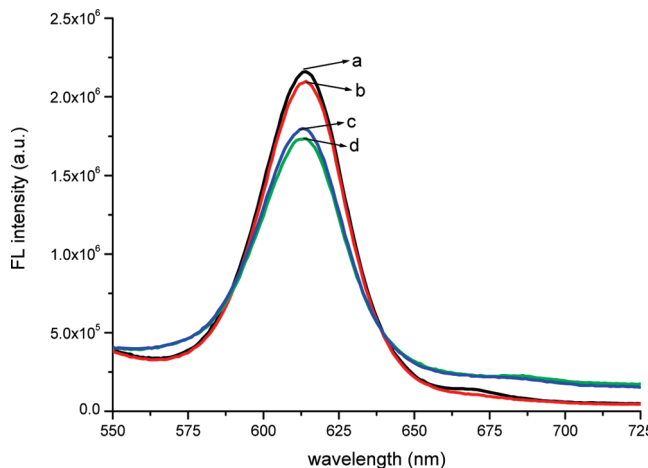


Figure 9. Test for the interference of different pyrethroids on the fluorescence response toward LC of CdSe@SiO₂@MIP. (a) CdSe@SiO₂@MIP, (b) CdSe@SiO₂@MIP + interfering mixed pyrethroids, (c) CdSe@SiO₂@MIP + LC (d) CdSe@SiO₂@MIP + LC + interfering mixed pyrethroids. (10 $^{-4}$ mol L $^{-1}$ of LC and interfering pyrethroids were used, the interfering mixed pyrethroids: DM, CM, and PM).

acceptor, which introduces new nonradiative decay pathways for the excitation.³⁰

To obtain the binding affinity properties of specific imprinted binding sites (CdSe@SiO₂@MIP) and non-specific sites (CdSe@SiO₂@NIP), the fluorescence titration analysis has been carried out. The quench amount between the fluorescent intensities of the imprinted receptor (CdSe@SiO₂@MIP and CdSe@SiO₂@NIP) at a given related pyrethroids (LC and CM) concentration and in a pyrethroids free solution is taken as equal as the uptake amounts. Figure 10 shows that the quench amount of binding LC by imprinted nanospheres increases significantly with the concentrations of LC in solution (■). However, the nonimprinted nanospheres did not exhibit the obvious difference in the rebinding capacities of LC (●) and CM (▼).

Determination of Pyrethroids. The FL intensity of the CdSe@SiO₂@MIP turns out to be decreased sensitively in the presence of LC in 50% (v/v) ethanol–water solution. The silica shell was used to provide functional groups (NH₂) that interact with the template LC via hydrogen bond (as shown in Figure 2) during the synthesis process. When the LC was removed by solvent extraction, imprinted binding sites (cavity) were left in

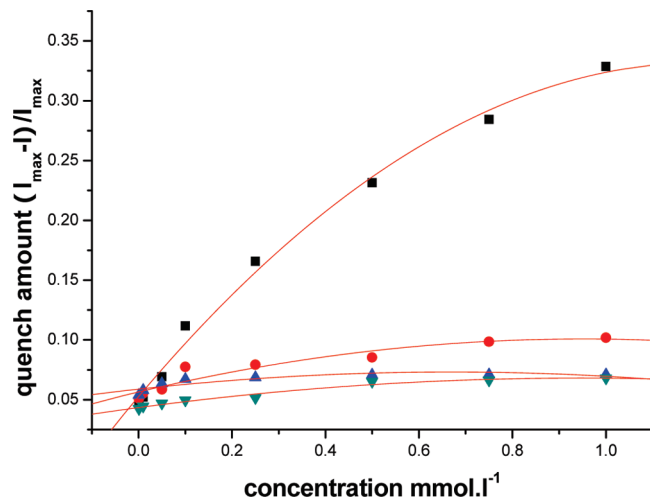


Figure 10. Comparison of molecular recognition properties. The amounts of LC molecules bound by (black squares) CdSe@SiO₂@MIP and (blue up-pointing triangles) CdSe@SiO₂@NIP and the amounts of CM molecules bound by (red circles) CdSe@SiO₂@MIP and (purple down-pointing triangles) CdSe@SiO₂@NIP.

the nanoparticles materials that are capable of selectively rebinding the target molecule LC. Figure 11 show the effect of increasing concentrations of LC on the fluorescence of the CdSe@SiO₂@MIP. As shown in previous literature, the analyte quenches the QD chemosensor in concentration dependence which accords with the Stern–Volmer equation have been reported by Rosenzweig's group and Yan's group, and so forth.^{3,21} In fact, these studies indicate the quenching mechanism deviates from Stern–Volmer behavior but accords with Stern–Volmer equation. For this reason, it is found that the quenching fluorescence of the CdSe@SiO₂@MIP in a concentration of LC dependence that can be described by a Stern–Volmer type equation:

$$I_{\max}/I = 1 + K_{\text{SV}}[S]$$

I and I_{\max} are the fluorescent intensities of the CdSe@SiO₂@MIP at a given related LC concentration and in a LC free solution, respectively. K_{SV} is the Stern–Volmer quenching constant, and $[S]$ is the LC concentration. The dependence of I_{\max}/I as function of $[S]$, are shown in Figure 11. The K_{SV} are found to be 4594 M $^{-1}$. The linear range of the calibration curve is 0.1–1000 $\mu\text{mol L}^{-1}$. The detection limit (DL), calculated following the 3 σ IUPAC criteria, is down to 8.0 nM (3.6 $\mu\text{g} \cdot \text{L}^{-1}$), which achieved the level of the current chromatographic techniques detection. For example, Liu and co-workers used HPLC for determination of pyrethroids with DL of 10–17 $\mu\text{g} \cdot \text{kg}^{-1}$.²⁵ Lentza-Rizos group also reported that gas chromatography with electron-capture detection (GC-ECD) have been used for detection several pyrethroids with DL in a range of 20–50 $\mu\text{g} \cdot \text{kg}^{-1}$.³¹ In addition, the luminescence method does not require large solvent consumption, time-consuming and tedious sample pretreatment;

(30) Helgeson, R. C.; Mazeleyrat, J. P.; Cram, D. J. *J. Am. Chem. Soc.* 1981, 103, 3929–3931.

(31) Lentza-Rizos, C.; Avramides, E. J.; Visi, E. *J. Chromatogr. A* 2001, 921, 297–304.

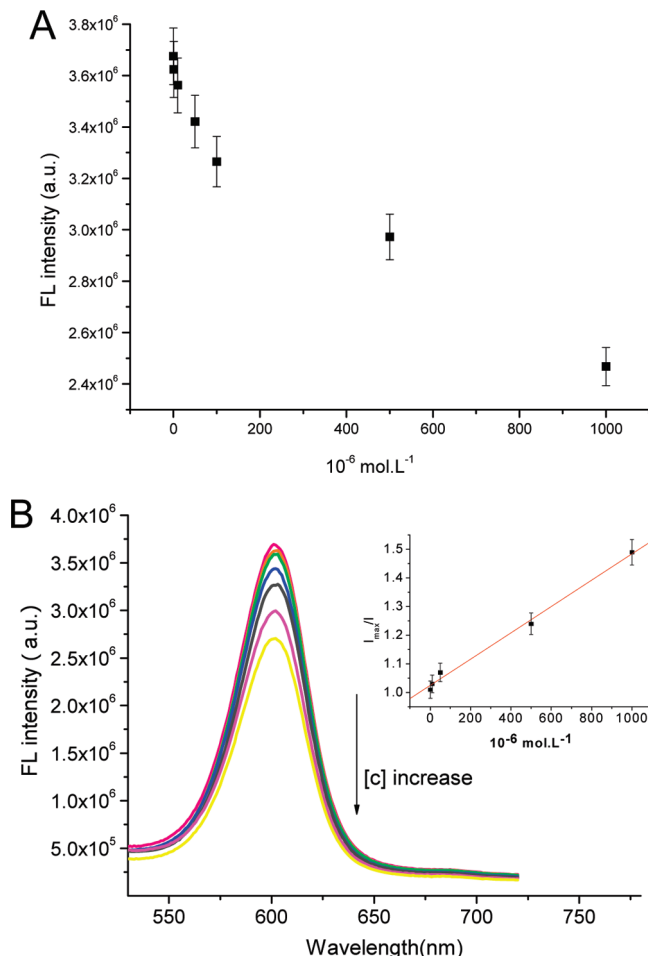


Figure 11. (A) Effect of LC concentration on the FL intensity of CdSe@SiO₂@MIP, (B) fluorescence spectra of the MIPs with the increasing concentrations of LC. Inset: Stern–Volmer-type description of the data showing a linear fit throughout the LC concentration range, with a correlation coefficient = 0.997.

therefore, the luminescence analysis is more suitable for the on-site and rapidly detect analysis.

Application to Water Sample Analysis. Surface river water samples were collected from local rivers. The samples were filtered through 0.45 μm Supor filters and stored in precleaned glass bottles. As no pyrethroids in the collected water samples were detectable by the proposed method, a recovery study was carried out on the samples spiked with 0.1–5 $\mu\text{mol L}^{-1}$ LC to evaluate the developed method. LC solutions were tested by CdSe@SiO₂@MIP, and focusing on the linear regime of fluorescence changes versus concentration permitted the construction of a “standard” curve to which our data were compared (Figure 11). From this curve and the fluorescence recovery measured for the unknown samples, we were able to derive estimates of LC levels in the water

Table 2. Recovery of LC in Water Samples with LC Solution at Different Concentration Levels

	concentration taken ($\mu\text{mol L}^{-1}$)	found ($\mu\text{mol L}^{-1}$)	recovery (%)
LC	5	4.95	99
LC	1	1.02	102
LC	0.5	0.48	96
LC	0.1	0.98	98

sample collected from local river. A summary of the calculated mean LC concentration for each water sample from the fluorescent assay and the corresponding result is shown in Table 2. The recoveries were from 96% to 102%. The values determined by the CdSe@SiO₂@MIP show the ability of our QD sensing assembly to provide accurate measures of LC concentrations in unknown environmental samples. It can be used for the direct analysis of relevant real samples.

Conclusion

A simple method for the formation of molecular recognition sites on the surface of silica nanospheres embedded CdSe QDs was developed. The silica shell was used to provide functional groups that interact with the template during the synthesis process. When the template was removed by solvent extraction, imprinted binding sites were left in the nanoparticle materials that are capable of selectively rebinding the target molecule. The synthesized CdSe@SiO₂@MIP is employed as a novel and highly sensitive luminescence probe for optical recognition of LC. Quenching of the luminescence emitted by the synthesized nanoparticles allows the determination of LC as low as 3.6 $\mu\text{g L}^{-1}$. In view of the sensitivity and the selectivity, the synthesized nanospheres afford a very sensitive detection system for pesticides analysis. Furthermore, molecular recognition of CdSe@SiO₂@MIP is in progress in our laboratory, which should spark a broad spectrum of interest because of its great versatility and flexibility for future applications.

Acknowledgment. This work was financially supported by the National Natural Science Foundation of China (20772038), 863 program (2009AA06A417), Program for Excellent Research Group of Hubei Province (2009CDA048), Self-determined research funds of CCNU from the colleges’ basic research and operation of MOE (CCNU09AO200).

Supporting Information Available: The fluorescence spectra of CdSe QDs and CdSe@SiO₂@NIP with different emission. TEM and SEM images of CdSe@SiO₂@LC. The photon correlation spectroscopy of CdSe@SiO₂@NIP and CdSe@SiO₂@MIP. This material is available free of charge via the Internet at <http://pubs.acs.org>.